TOPICAL REVIEW

Basis and effects of ion migration on photovoltaic performance of perovskite solar cells

To cite this article: Wenke Zhou *et al* 2021 *J. Phys. D: Appl. Phys.* **54** 063001

IOP Publishing Journal of Physics D: Applied Physics
J. Phys. D: Appl. Phys. **54** (2021) 063001 (16pp) https://doi.org/10.1088/1361-6463/abbf74

Topical Review

Basis and effects of ion migration on photovoltaic performance of perovskite solar cells

Wenke Zhou[1,2], Juan Gu[2], Zhiqian Yang[2], Mingyang Wang[2] and Qing Zhao[1,3,4]

[1] State Key Lab for Mesoscopic Physics and Frontiers Science Center for Nano-optoelectronics, School of Physics, Peking University, Beijing 100871, People's Republic of China
[2] Army Engineering University of PLA, State Key o Laboratory for Disaster Prevention & Mitigation of Explosion & Impact, Nanjing 210007, People's Republic of China
[3] Peking University Yangtze Delta Institute of Optoelectronics, Nantong 226010, Jiangsu, People's Republic of China
[4] Collaborative Innovation Center of Quantum Matter, Beijing 100084, People's Republic of China

E-mail: zhaoqing@pku.edu.cn

Received 21 July 2020, revised 13 August 2020
Accepted for publication 8 October 2020
Published 11 November 2020

Abstract

Halide perovskite materials, which are emerging as some of the most promising candidates for photovoltaics, have been widely studied and have been certified as demonstrating a comparable efficiency to single-crystal silicon solar cells. However, their low stability poses a challenge for commercialization. External impediments, like moisture, heat, and UV light, can be addressed by strict encapsulation; nevertheless, ion migration remains. The migrated ions will bring in a growing number of charged defects and phase segregation to bulk perovskite; they will cause interfacial band doping and degradation of the carrier transport layer, which will greatly hinder carrier transportation. Those effects are the origins of perovskite intrinsic instability. Thus, a thorough understanding of the operational mechanism of ion migration is urgent for the fabrication of perovskite solar cells (PSCs) with improved stability. Here, we systemically summarize the factors governing ion migration in perovskite film and the associated impact on the performance of PSCs. Light illumination, organic cations, grain boundaries, residue lattice strain and moisture have been found to make ion migration easier. Strategies developed to suppress the ion migration are also interspersed in each section.

Keywords: perovskite solar cells, stability, ion migration, photovoltaic performance

(Some figures may appear in color only in the online journal)

1. Introduction

Organic–inorganic metal halide perovskite materials have been demonstrated to have excellent physical/chemical properties [1–6] and have a certified power conversion efficiency (PCE) of 25.2% for perovskite solar cells (PSCs) [7]. Additionally, the low temperature solution fabrication process (<150 °C) [8–10] and adjustable bandgap [11–16] make it compatible with the fabrication of tandem devices [17, 18]. However, instability issues hider the commercialization of PSCs [19, 20]. When performing stability tests, PSCs could degrade under light and applied voltage; even the perovskite film shows no obvious sign of decomposition [21]. Therefore, the instability of PSCs has two aspects: intrinsic and nonintrinsic. Intrinsic instability is described as the device degradation under light and electric field, excluding the influence

of external factors, such as moisture [22], oxygen [23], heat [24] and UV light [25]. Accordingly, external factors-induced instability, which could be addressed by model encapsulation, is nonintrinsic.

Thus, for PSCs, intrinsic instability is the most urgent problem needing to be solved. Apart from the photothermic-induced decomposition, perovskite crystal contains a large amount of weak ionic bonds [26], a feature that makes ion migration possible. In 2014, Xiao *et al* first gave a robust proof for ion migration in perovskite film through an optical microscope; and found the ion migration-induced band doping effect via utilizing Kelvin probe technology [27]. Since then, ion migration has received extensive attention. Anomalous phenomena, such as giant dielectric constant at low frequency [28], light-induced phase segregation [29] and the light-induced self-poling effect [30], and photocurrent–voltage hysteresis [31] were discovered to be correlated with ion migration. Under the electric field, charged ions could migrate. From bulk inside to electrodes, along the migrating channels, ions cause increased defect state densities and interfacial polarization, finally leading to device performance degradation. Therefore, a systemic and comprehensive understanding of ion migration in perovskite materials is urgently desired.

In this review, we will provide a survey of research to highlight the most pressing concerns regarding ion migration, ranging from fundamental physical properties to kinetic characterization. We will focus on the following issues: (1) basic understanding of ion migration: evidence and migrating species; (2) influence of ion migration on device performance; (3) factors that can enhance ion migration: light, perovskite composition, perovskite grain boundary (GB), lattice strain, and moisture. Each section will be discussed from a mechanistic point of view, from which suggestions are provided to suppress the associated ion migration for improved photovoltaic performance, especially the operational stability of PSC devices.

2. Basis of ion migration in perovskite

In 1983, inorganic perovskites ($CsPbCl_3$, $CsPbBr_3$ and $KMnCl_3$) were proved to be halide-ion conductors [32], in which the ion conduction was considered to have arisen from the migration of halide-ions vacancies. For hybrid perovskite such as $CH_3NH_3PbI_3$ ($MAPbI_3$), the first question is to obtain the direct evidence of ion migration, then figure out the migrating species in the film.

2.1. Evidence of ion migration in perovskite film

Xiao *et al* first demonstrated a giant switchable photovoltaic effect in a perovskite device with an Au/perovskite/PEDOT:PSS/ITO vertical structure and symmetric electrode working functions (−5.4 eV for Au and −5.3 eV for PEDOT:PSS). During the voltage scanning process the direction of photocurrent was completely reversed [27] (figure 1(a)). Additionally, in an Au/$MAPbI_3$/Au lateral structure, the surface color of perovskite film at two electrodes changed significantly after extended electric poling of ∼1.2 V μm^{-1}, under an optical microscope (figure 1(b)). If no p–n junction formed in this device with a symmetric band structure, electrons and holes could not be efficiently separated by the built-in field, thus no current would generate. So poling-controlled switchable photocurrent provides the evidence for the existence of ion migration and implies that it could bring in interfacial band doping.

Later, Yang *et al* set up a solid-state electrochemical cell Pb|$MAPbI_3$|AgI|Ag (figure 1(c)), consisting of one electronic electrode (Pb electrode taken as '+') and one ionic electrode (AgI electrode taken as '−'), to investigate the chemical effects at various interfaces upon long-term charge transference [33]. Combining with a scanning electron microscopy (SEM) micrograph, energy dispersive x-ray spectroscopy (EDX) and x-ray diffraction (XRD) characterization (figure 1(d)), PbI_2 was detected at the Pb|$MAPbI_3$ interface. It demonstrated that I^- can easily migrate through $MAPbI_3$ film, and provided strong and compelling evidence for the presence of electric field-induced ion migration in $MAPbI_3$. In addition to $MAPbI_3$, similar switchable photocurrent phenomena were also reported in solar cells with different structures and perovskite components [34, 35]. Therefore, ion migration was general and intrinsic in organic–inorganic halide perovskite materials. Moreover, the timescale of those electrochemical changes is around a week, from which one can speculate that the ionic carrier mobility is much lower than that of electrons.

2.2. What is moving in perovskite film under electric field?

Given that perovskite crystals have low formation energies of point defects [36–40], any species such as MA^+, I^-, Pb^{2+} may migrate. In a solid-state material, the term 'activation energy' (E_a) was usually adopted to characterize the energy barrier that an atom needs to surmount before moving from one lattice site to another. Its value correlates with the ionic radius, hopping distance, electric charge and neighboring ions, in which a smaller E_a means a higher possibility of ionic motion. Several theoretical works, via first-principles methods, concluded that I^- is more ready to migrate in perovskite film. For example, in the work of Eames *et al*, iodine ions move along the I–I edge of the $[PbI_6]^{4-}$ octahedron with the activation energy of 0.58 eV (figure 2(a)). MA^+ migrates through the unit cell face surrounded by four I^- ions with a higher activation energy of 0.84 eV (figure 2(b)); and Pb^{2+} ions move along the <110> direction of the unit cell with the highest migration energy barrier of 2.31 eV [41]. Therefore, I^- was the majority mobile ions and its diffusion coefficient was estimated to be 10^{-12} cm^2 s^{-1} at 300 K. Due to the estimated diffusion coefficient, I^- can migrate through the perovskite film within 100 s, coinciding with the time scale of the *I–V* hysteresis in $MAPbI_3$ film [42]. Therefore, ion migration was considered to be the main origin for *I–V* hysteresis in PSCs. Similarly, Haruyama *et al* calculated an energy barrier of around 0.33 eV for I^- and 0.55 eV for MA^+, indicating that MA^+ and I^- are freely diffusible at room temperature [43]. We should be aware that the existing calculations only involve the ion migration via the hopping

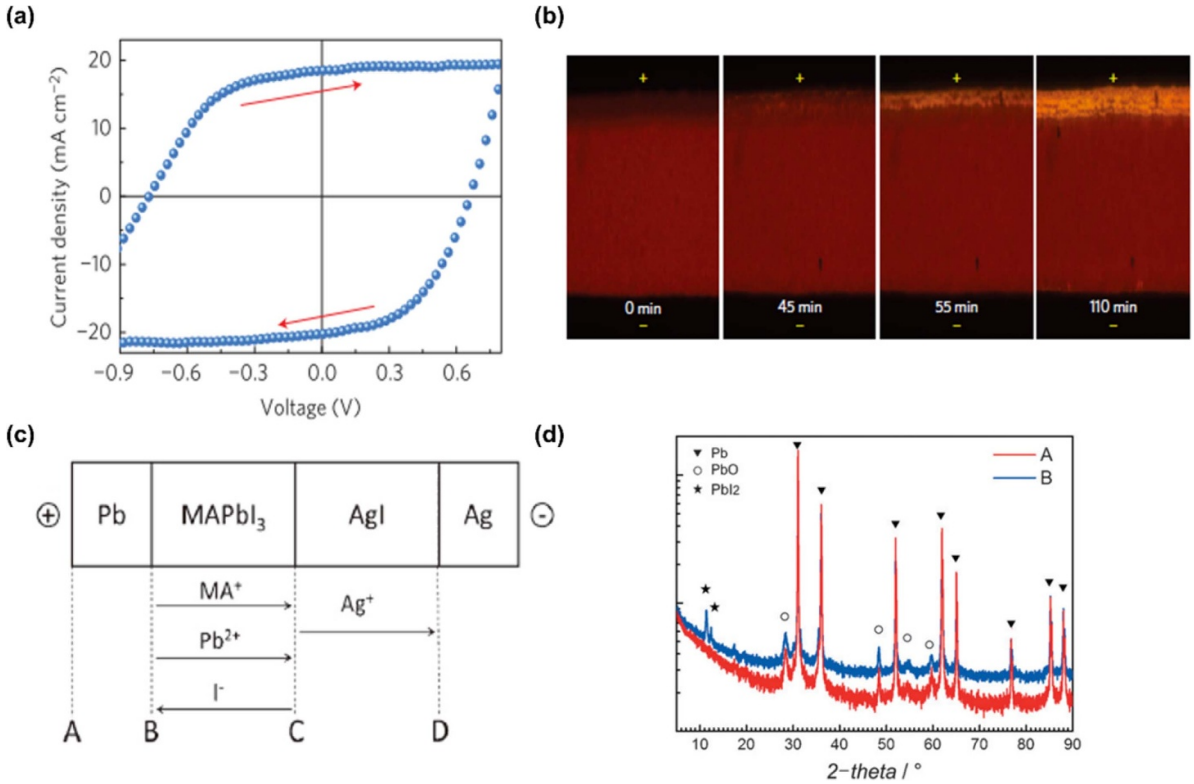

Figure 1. (a) $J-V$ curves of the Au/perovskite/PEDOT/ITO devices under continuous current sweeping at a rate of 0.14 V s^{-1} between −2.5 V and 2.5 V. The arrows in the figures show the scanning direction. (b) Snapshots of the *in situ* recorded video for monitoring the poling process using a lateral structure device. Reprinted with permission from Springer Nature Customer Service Centre GmbH: Nature Materials [27], 2014. (c) Flow directions of the charged ion species in a Pb|$MAPbI_3$|AgI|Ag cell under electrical bias. (d) XRD patterns of surfaces A and B of the Pb disk after applying a DC current of 10 nA for a week. [33] John Wiley & Sons. © 2015 WILEY-VCH Verlag GmbH & Co. KGaA, Weinheim.

of vacant ions in bulk crystal. Therefore, theoretical analysis, based on interstitial defects and GB-dominated ion migration, is highly desired.

In order to find direct evidence of ion migration, Yuan *et al* applied photothermal-induced resonance (PTIR) microscopy to map the spatial distribution of MA^+, before and after electric poling on a lateral $MAPbI_3$ device [44] (figure 2(c)). After exerting a moderate electric field of 1.6 V μm^{-1} for 100 s–200 s, the PTIR signal intensity indicated a redistribution of MA^+ in the perovskite film, robustly proving the electromigration of MA^+. Then, via Kelvin probe force microscopy (KPFM) characterization (figure 2(d)), Yuan *et al* observed a reversible electric field-driven conversion between $MAPbI_3$ and PbI_2 at an elevated temperature of 330 K [45], which could be explained by a massive migration of MA^+ and I^-.

Besides I^- and MA^+, hydrogenic impurities (H^+, H^0 and H^-) are also predicted to exist in $MAPbI_3$ by Egger *et al* [46]. The hydrogenic impurities can be generated during the decomposition process of $MAPbI_3$ crystal or from the deprotonation process of MA^+ cation. And according to density functional theory (DFT) calculations, the activation energy for H^+ hopping along the I–I path is around 0.17 eV to 0.29 eV [46], depending on the extent of lattice relaxation, which implies that hydrogenic impurities are general and ready to move. Thus, except for the 'heaviest' Pb^{2+} ions, the rest of the species of $MAPbI_3$ can all migrate and lead to an anomalous effect in perovskite film and solar cells.

3. How ion migration influences perovskite film and solar cells

Due to experimental and theoretical results, ions could migrate in perovskite film at an electric field of 0.3 V μm^{-1} or even smaller [45–47], and cause a switchable photovoltaic effect in a lateral device [44], with a relatively low activation energy [46]. This evidence strongly implies that ion migration occurs once the solar cells operate under electric field and light illumination, then induces defects in bulk and band doping at the interface, which finally makes the solar cells instable. Therefore, it is necessary to investigate the mechanism between device degradation and ion migration to fix intrinsic instability, then work towards highly stable PSCs.

3.1. Phase segregation and defect state formation

Hoke *et al* observed a reversible light-induced phase segregation in mixed-halide $MAPb(I_xBr_{1-x})_3$ in 2015 [29]. For the perovskite film with bromide concentrations exceeding 20%, they observed a photoluminescence (PL) red shift from a 1.9 eV to 1.68 eV in less than 1 min, under illumination lower than one

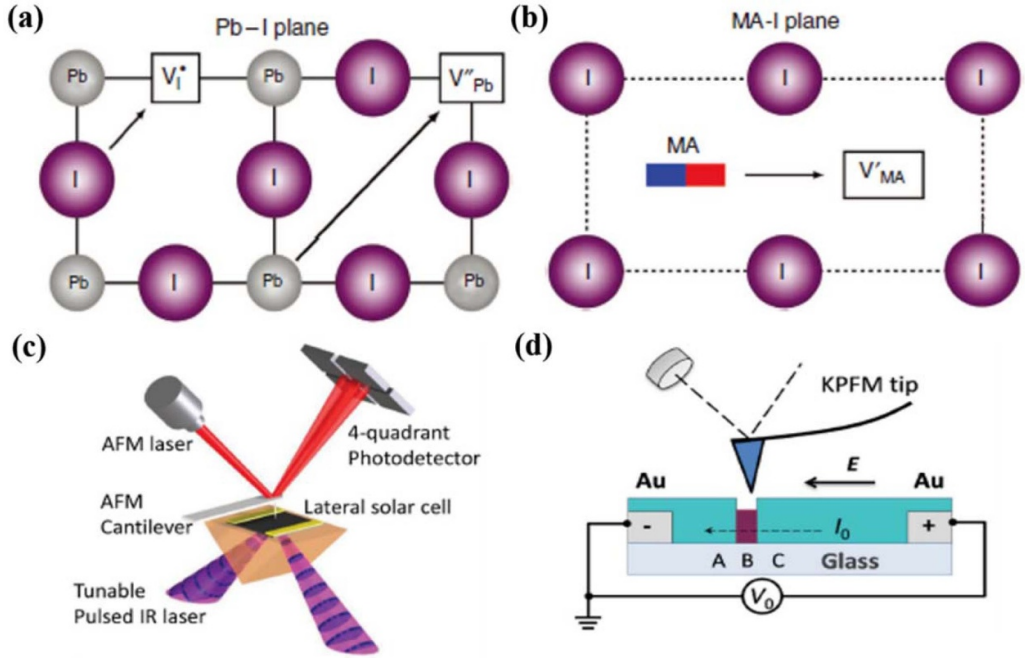

Figure 2. (a) Schematic illustration of the I^- transport mechanisms involving conventional vacancy hopping between neighboring positions. (b) MA^+ migration into a neighboring vacant A-site cage involving motion normal to the unit cell face composed of four iodide ions [41]. Reproduced from [41]. CC BY 4.0. (c) Schematic illustration of the PTIR measurement on $MAPbI_3$ film. [44] John Wiley & Sons. © 2015 WILEY-VCH Verlag GmbH & Co. KGaA, Weinheim. (d) Schematic illustration of the KPFM measurement around the PbI_2 thread. [45] John Wiley & Sons. © 2015 WILEY-VCH Verlag GmbH & Co. KGaA, Weinheim.

sun (15 mW cm^{-2}) at room temperature. Combined with XRD and absorption characterization, $MAPb(I_xBr_{1-x})_3$ was found to split into I-rich and Br-rich domains; in addition, after 5 min storage in darkness, the PL spectra recover to their original position, indicating different stable states for perovskite under light and dark. Further, Beal *et al* found a similar shift of PL spectra in $CsPb(Br_xI_{1-x})_3$ for $0.4 < x < 1$ [48]. The I-rich component perovskite, with a lower bandgap, could act as charge-trapping defects and lead to the reduction of open-circuit voltage (V_{oc}) in PSCs. The PL shift is usually observed after several seconds, the timescale close to that typically associated with ionic motion. Therefore, the phase segregation is thought to be related to ion migration, which needs more evidence.

Later, Zhao *et al* developed an integrated means, a combination of standard galvanostatic measurement [33] withan *in situ* PL scan and real-time optical microscopy recording, to monitor the ion migration in $MAPbI_3$ film [49] (figure 3(a)). This characterization was realized in a lateral setup (Au/$MAPbI_3$/Au), upon switching the current from zero to a constant small value (figure 3(b)). After the current is switched on, both electrons and ions contribute to conductivities. Due to the drive of electric field, ions gradually accumulated near two electrodes, and a screen field was gradually formed. Due to the blocking effect of accumulated ions, a larger voltage was required to maintain the constant current of the system. Finally, the voltage reached an equilibrium state when only electronic conductivities existed. Therefore, during the slow depletion process of mobile ions, any variation of the PL spectra and optical images can be related to the ion migration-induced effects [27, 45]. During electric poling, they found that the PL intensity decreased in several seconds both at the anode (figure 3(c)) and the cathode (figure 3(d)) after the current was switched on, illustrating that defect states increased across the perovskite film. Besides, an obvious blue shift around 10 nm occurred near the anode, which may have arisen from the band-filling effect induced by the iodine vacancies with n-doping [50, 51]. Further, a PL-mapping measurement was conducted on a 30 × 50 μm^2 area, to confirm ion migration could induce an entire change on perovskite film. As a result, the mapping data showed the largest PL intensity decay at two electrodes, coinciding with the result in line scan mode.

Then, in the I-Br mixed perovskite system, the PL peak position showed an approximately 30 nm red shift at the anode and a 50 nm blue shift at the cathode [52], providing strong evidence for halide redistribution. Additionally, DFT calculation results showed that, after electric poling, I trimers can form in the I-poor region while Pb dimers can form in the I-rich area [49] (figures 3(e)–(g)), introducing deep-level defects around 0.3 eV below the conduction band minimum. Therefore, ion migration-induced trap states can act as nonradiative recombination centers in perovskite film, decrease the charge carrier lifetime, and cause solar cell degradation. Accordingly, lowering the defect state densities is vital to inhibit the ion migration inside the perovskite bulk crystal.

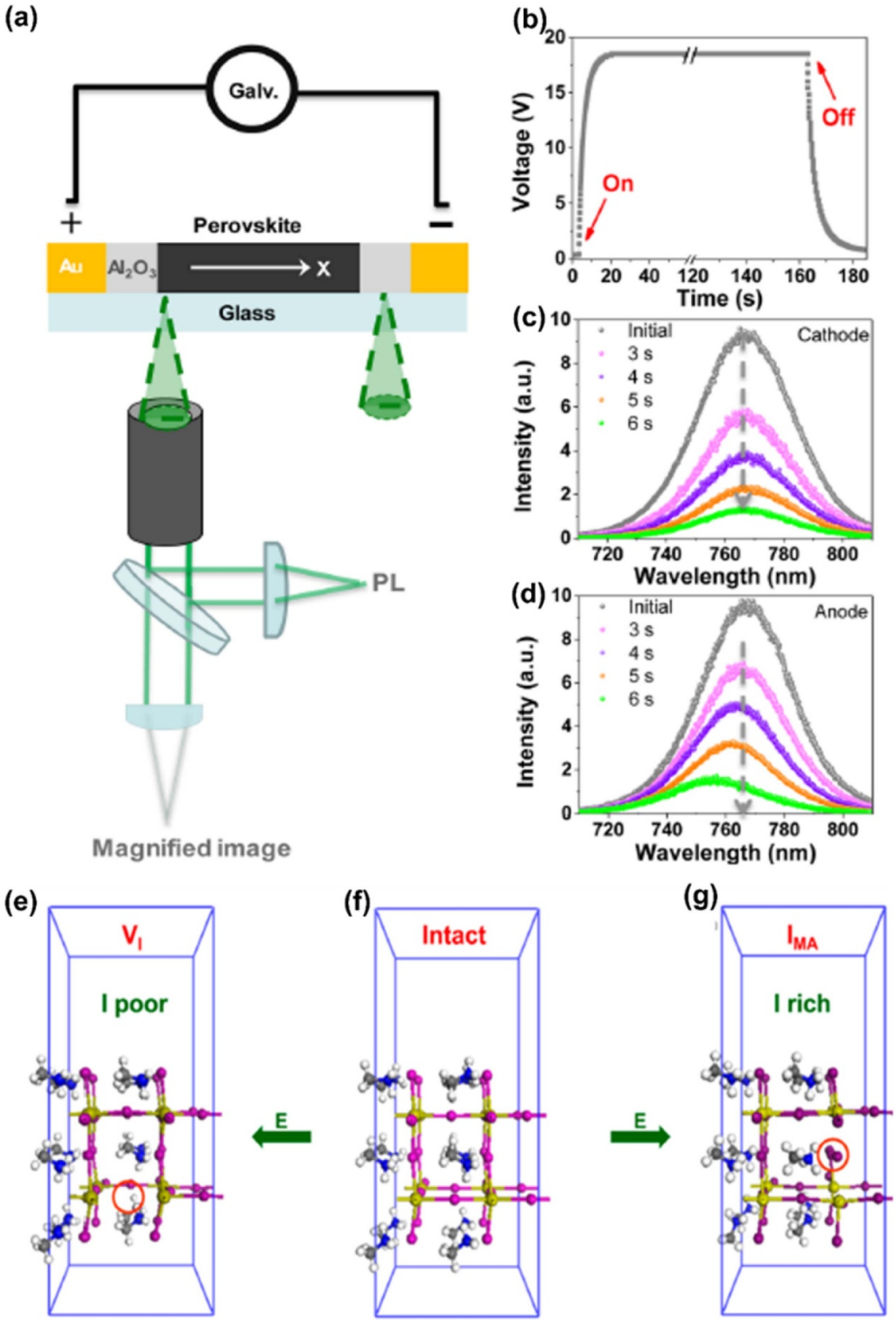

Figure 3. (a) Schematic illustration of the *in situ* PL characterization with galvanostatic measurement. (b) Voltage–time (*V*–*t*) curve for a fixed direct current at 10 nA. The 'on' and 'off' indicate the current switches on and off, respectively. (c) PL spectra show a significant decrease at the positive pole (cathode) after electric poling at 1 V μm^{-1} for 6 s. (d) PL spectra show a significant decrease at the negative pole (anode) after electric poling at 1 V μm^{-1} for 6 s, accompanied by a strong blue shift from ∼765 to 757 nm. (e)–(g) Atomic structure of 2D perovskite $(CH_3NH_3)_3Pb_2I_7$ viewed along the direction perpendicular to the *z*-axis. Color scheme: Pb: gold; I: purple; C: dark gray; N: blue; H: white. (f). Red circles in (e) and (g) represent the I trimer and Pb dimer, respectively. Reproduced with permission from [49]. Copyright 2016 American Chemical Society.

3.2. Ion accumulation-induced interfacial band doping

Besides the photoactive layer, interface plays a vital role in charge carrier transportation in photovoltaic devices [53–59], and migrated ions could influence this process due to progressively interfacial accumulation. In the early works reported by Xiao *et al*, a giant switchable photovoltaic effect can generate in a symmetrical solar device under electric poling (<1 V μm^{-1}) and light illumination [27]. This means that accumulated ions in the perovskite near the electrodes can induce p-type and n-type doping, respectively. Theoretical works had predicted that positively charged iodine vacancies or MA^+ interstitials can cause n-type doping while the negatively charged MA^+ vacancies or I^- interstitials can cause p-type doping [38, 60]. To verify this scenario, KPFM characterization was conducted on an Au/Perovskite device with part of Au electrode peeled off. The potential images indicated that, when the positive charged ions move towards cathode, it will result in a p-i-n structure (figures 4(a)) and a reverse bias can flip it to n-i-p (figure 4(b)). During this process, surface topography showed no obvious change in the poling areas, thus ruling out the influence of topography on the surface potential characterization. Thus, accumulated ions could bring in defect states at interface and cause band-bending, which would hinder the charge transportation then attenuate the device stability. Due to the planar heterojunction structure of PSCs, interfaces may be more sensitive to accumulated ions, in comparison to bulk crystal, which were reported to have a substantial tolerance to point defects. Thus, interface passivation is highly desired for long-term stable PSCs.

3.3. Ion penetration-induced degradation of organic hole-transport layer

In highly efficient PSCs, the most common organic hole-transport layers (HTLs) consist of 2,2′,7,7′-tetrakis (N,N-di-4-methoxyphenylamino)-9,9′-spirobifluorene (spiro-OMeTAD) [62, 63], poly(triarylamine) (PTAA) [64, 65], or their derivatives. Due to the soft organic nature of spiro-OMeTAD, part of the accumulated ions can pass through the perovskite/HTL interface then penetrate into the HTL layer. Zhao *et al* systemically investigated the mobile MA^+ induced degradation of organic HTL [61]. Initially, they measured XRD patterns of perovskite films in fresh and degraded devices (operation for 8 min in air with ∼35% humidity), which showed no appearance of excess PbI_2, indicating that negligible decomposition occurs in the perovskite films. Then by replacing the spiro-OMeTAD layer in the degraded cells with a fresh film, the cell efficiency increases from 4.9% (degraded cell) to 11.2% (recovered cell), with the initial PCE of 16.1% in the fresh cell. This efficiency recovery means that the degradation of the HTL layer should be responsible for part of the efficiency loss. Then the time-of-flight secondary-ion mass spectrometry clearly showed that, in the degraded devices, there was a conspicuous overlap between the MA^+ and spiro distribution (figure 4(d)), much larger than that in the fresh cell (figure 4(c)). This provided strong evidence for MA^+ penetration into the HTL, which can be explained by the MA^+ migration under electric field and illumination (figure 4(e)). Combining the impedance spectra analysis of solar cells at different statuses (initial, degraded, replaced with new HTL), they found that additional MA^+ can increase the defect states densities in HTL and then lead to the degradation of solar cells. To improve the device resistance against MA^+ penetration, applying inorganic hole-transport material is an option, considering the robust covalent bonds in inorganic crystal; in addition, an ion-blocking layer could be inserted between the perovskite/HTL interface. However, in our view, finding a stabilizer to inhibit ion migration from the origin, namely in perovskite crystal, and combining it with interface passivation, are the top priorities.

4. Which factors can affect ionic motion?

In work reported by several groups, the relaxation time of ion migration in perovskite film varied by several orders of magnitude [49, 66, 67], even under the same electric poling condition. Crystal quality and the surrounding environments could be the invisible hands, regulating the ionic motion behavior. Therefore, figuring out which factors affect ionic motion, then obtaining a clear map of the PSCs' operational mechanism, is the ticket to improved device stability.

4.1. Moisture

In 2015, Leijtens *et al* investigated how water molecules affect the ionic motion in $MAPbI_3$ film [68]. Under 30% humidity, by applying an electric filed of around 0.06 V μm^{-1}, the bare perovskite film exhibits an extremely quick and irreversible degradation (figure 5(a)). Then, Zhao *et al* found that, when coating with a PMMA layer, the $MAPbI_3$ film slowly, over hours, turned into a yellow phase. In addition, the film shows no obvious change in vacuum condition [49] (figure 5(b)). In typical PSCs, the built-in field is around 1 V μm^{-1}, which is two orders of magnitude higher than that used in Leijtens's experiment. The above experimental results strongly suggest that humidity can greatly enhance ion migration. The possible mechanism for moisture-enhanced ion migration can be described as: once the water molecules (H_2O) absorb on the surface of perovskite crystal, hydrogen bonding will form between H_2O and organic cation (MA^+ or FA^+). The external disturbance may reduce the interaction between MA^+/FA^+ and the surrounding $[PbI_6]^{4-}$ octahedron, then lower the energy barrier for MA^+/FA^+ migration [68]. Therefore, applying an inert environment in the fabrication process, combined with strict encapsulation, is vital to isolate the PSCs from water molecules for better stability.

4.2. Light illumination

Perovskite devices can maintain their original performance after several months' storage in darkness in an inert gas environment; however, they exhibit fast decay under light [21, 70, 71]. To get further insight into how light affects perovskite film, Zhao *et al* investigated the variation of perovskite morphology under different light intensities via

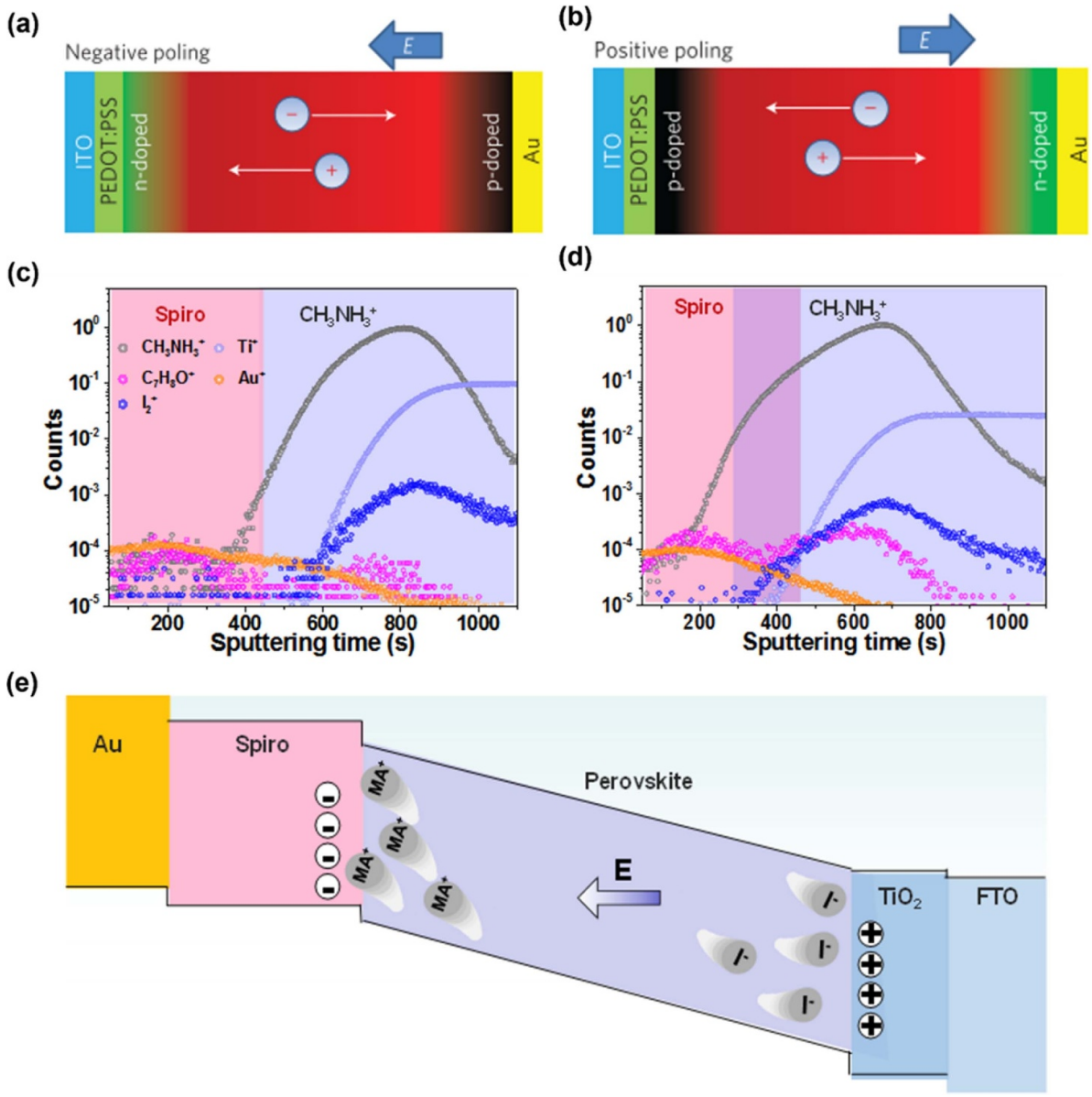

Figure 4. (a), (b) Schematics of ion drift in perovskite during positive and negative poling, respectively, showing that accumulated ions in the perovskite near the electrodes induced p-doping and n-doping. Reprinted by permission from Springer Nature Customer Service Centre GmbH: Nature Materials [27], 2014. (c), (d) Counts versus sputtering time by ToF-SIMS for different ions in the Au/HTL/perovskite/TiO_2/FTO architecture in (c) fresh cells and (d) degraded devices with over 60% efficiency loss. (e) Schematic of the electric field distribution in PSCs and the corresponding direction of ion migration. Reproduced with permission from [61]. Copyright 2017 American Chemical Society.

a Au/$MAPbI_3$/Au device structure by optical microscope [69]. After applying electric poling, they found that, when the illumination intensities increased, a growing number of pinholes and dendrites (PbI_2) emerged in the perovskite film (figure 5(c)). After comparing the element distribution in perovskite film before and after electric poling, a possible mechanism could be deduced: under the electric field and stronger light, massive numbers of I^- migrated towards the cathode and volatilized as I_2; MA^+ evaporated away in the form of CH_3NH_2 gas during the migration process from cathode to anode; and the $MAPbI_3$ gradually turn into PbI_2 phase. That is to say, light can enhance ion migration.

Then, the next question is to investigate the mechanism of light-enhanced ion migration in $MAPbI_3$ film. One prediction is that light can stimulate the attempt frequencies of ion migration [72–74] and another is that the photocrystal interaction can reduce the energy barrier for ion migration [75, 76]. To quantitatively evaluate the activation energy for ion migration, Zhao *et al* conducted cryogenic galvanostatic measurements to obtain the temperature-dependent ionic conductivities [32, 77, 78] under different light intensities. For solid-state mixed conductors, mixed conductivities σ_{tot} could be extracted by a current–voltage scan at a fast scan rate. Since a voltage (−10 V to 10 V) at 50 V s^{-1} was applied on the film with 50 μm width, the scanning period was short enough before

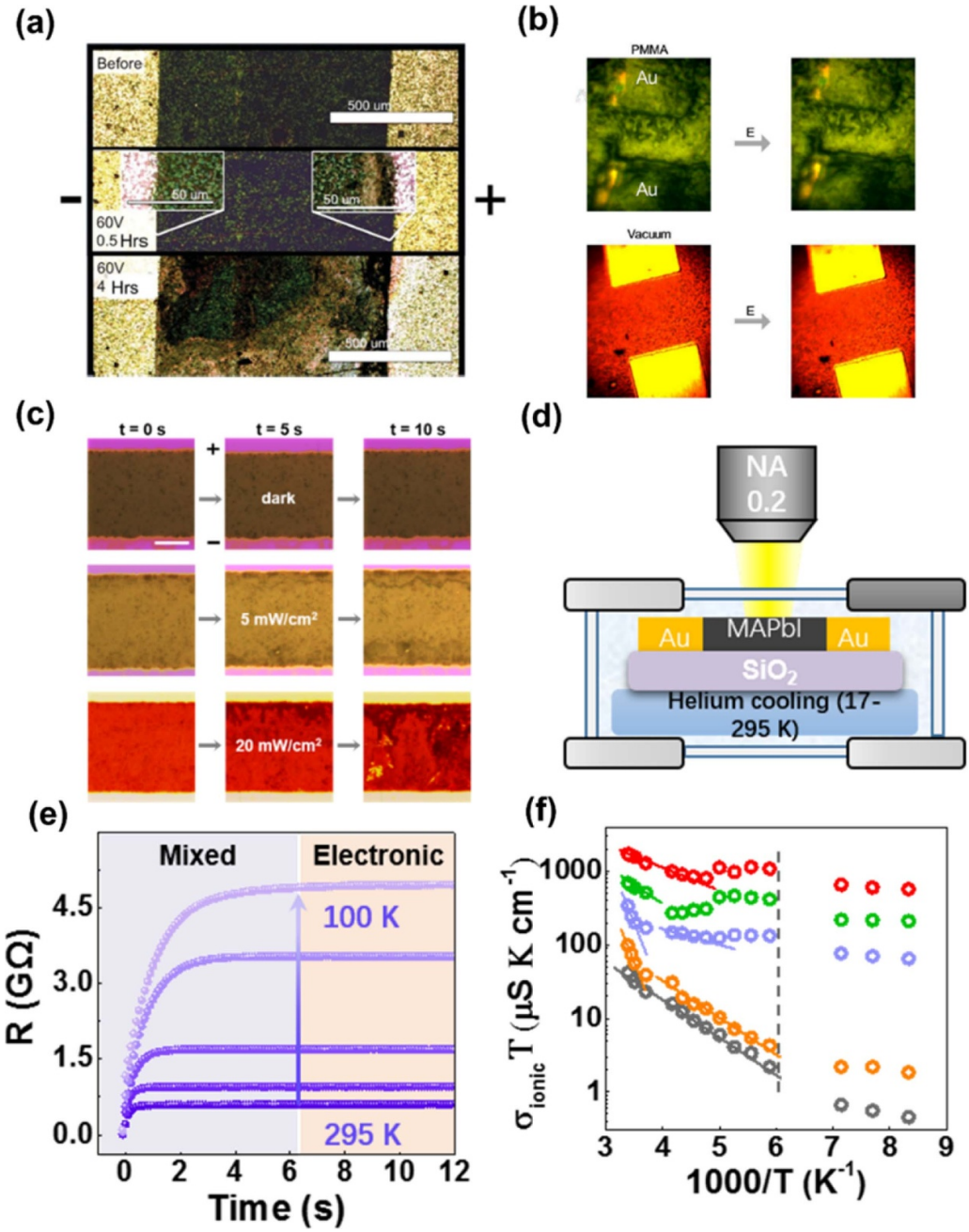

Figure 5. (a) Microscope images of the lateral different stages of electric field induced degradation in ∼30% humidity. [68] John Wiley & Sons. © 2015 WILEY-VCH Verlag GmbH & Co. KGaA, Weinheim. (b) Optical images change after 1 min high-field poling (1 V μm^{-1}), for the perovskite film with PMMA coating in ambient air and without any coating in vacuum. Reprinted with permission from [49]. Copyright 2016 American Chemical Society. (c) Optical dynamic images of perovskite film under electric poling and illumination of various intensities in ambient air at room temperature. The scale bar represents 20 μm. (d) The apparatus used in cryogenic galvanostatic measurement, with a helium cooling system. (e) Five typical galvanostatic curves recorded at different temperatures under a 20 pA current and 1 mW cm^{-2} illumination. (f) Ionic conductivity multiplied by temperature (from 17 K to 295 K), $\sigma_{ion}T$, as a function of 1000/T under various illumination intensities (grey: 0 mW cm^{-2}; orange: 0.05 mW cm^{-2}; purple: 1 mW cm^{-2}; green: 5 mW cm^{-2}; red: 20 mW cm^{-2}). The dashed line indicates the phase transition temperature. Reproduced from [69]. CC BY 4.0.

the full relaxation for ionic motion accomplishment. Therefore, the ionic accumulation in perovskite film during an I–V scan is negligible.

In order to separate ionic σ_i and electronic conductivities σ_e, Zhao *et al* conducted galvanostatic characterization with a tiny current, on the Au/$MAPbI_3$/Au with a helium cooling system (figure 5(d)). First, the current was switched on from zero to 20 pA. Then they measured the voltage of the structure as a function of time. The measured voltage reached an initial value, to which both electrons and ions contribute, and then gradually increased due to the screening effect of accumulated ions at two electrodes. The mobile ion was gradually depleted,

and finally, only electronic conductance remains (figure 5(e)). Ultimately, ionic conductance was extracted by subtracting the electronic conductance from mixed conductance under different temperatures and light intensities. Due to the hopping-like transport mechanism for ionic transport, the formula describing the energy barrier can be written as [32]:

$$\sigma_{\text{ion}}(T)T = ne\mu = \frac{Z_i e^2 N_A C_{v0} D_0}{k_B V_m} \exp\left(-\frac{G_v}{5k_B T}\right) \exp\left(-\frac{E_a}{k_B T}\right) = \sigma_0 \exp\left(\frac{-E_a^{\text{eff}}}{k_B T}\right),$$

in which Z_i stands for the ionic charge, N_A stands for Avogadro's constant, C_v stands for the concentration of intrinsic defects, k_B stands for the Boltzmann constant, V_m stands for the molar volume of perovskite, D stands for the diffusion coefficient, G_v stands for the formation energy for vacancy defects, and $E_a{}^{\text{eff}}$ stands for activation energy for ionic diffusion considering an additional vacancy formation energy. The fitting results (figure 5(f) and table 1) indicated that, with stronger light illumination, the activation energy for ion migration significantly reduced. That is to say, ions are easier to migrate under light. Similarly, deQuilettes *et al* reported the light-induced PL 'brightening' and halide redistribution of perovskite film [79]; Xin *et al* also found light-promoted ionic motion with a reduced energy barrier for ion migration [80]; and Kim *et al* discovered that the ionic conductivity of $MAPbI_3$ was enhanced by several orders of magnitude under light excitation [81].

Then by carefully analyzing the zoom-in view of temperature-dependent ionic conductance, the activation energy region shows two separate parts (figure 5(f)): E_{a1} ($T > 250$ K) and E_{a2} (180 k $< T <$ 250 K). Published results of E_a for I^- and MA^+ varied from 0.1 eV to 0.8 eV. For H^+, the activation energy was predicted to be ~0.17 eV or even smaller, if considering the nuclear quantum tunneling effect. Thus the E_{a1}, ranging from 0.14 eV to 0.82 eV, corresponds to I^- or MA^+, where the E_{a2}, from 0.06 eV to 0.13 eV, can only be assigned to H^+. However, in order to verify the existence of hydrogen migration, more direct evidence is needed.

Since the ionic transport had a timescale of several seconds in the galvanostatic test, the dynamic of ion migration could be analyzed by extracting the temperature-dependent relaxation time (kinetic constant) [82] (figure 6(a)). Below 80 K, the $\ln(K_{\text{ion}})$ of $MAPbI_3$ exhibits a T-independent behavior (figure 6(b)), which should be related to the deep quantum tunneling of the ions rather than conventional classical hopping. Owing to the light mass of H, H^+ is the most likely ions with which this tunneling can happen [46]. Then theoretical calculation predicted that the driving force for hydrogen migration gradually transforms from classical hopping ($T > 140$ K), through shallow quantum tunneling (140 K $> T >$ 75 K), to deep quantum tunneling ($T <$ 75 K), by applying *ab initio* path-integral molecular dynamic methods by Feng *et al* [82]. However, when the target perovskite changes to $CsPbI_2Br$, without H, the $\ln(K_{\text{ion}})$ ascends until the lowest temperature (figure 6(c)). Thus, for $CsPbI_2Br$, no quantum tunneling existed. Therefore, both experimental and theoretical work powerfully indicate that the horizontal lines below 80 K in figure 6(b) are intrinsic to H^+ migration in $MAPbI_3$. Hydrogen migration is not like I^- or MA^+, too light/tiny to be observed in classical mechanics. The above results highlight the novelty of this cryogenic-galvanostatic experiment, from which we can conclude the migration scenarios to have a deeper understanding of ion migration in perovskite.

4.3. Perovskite component

Understanding which ions are responsible for the light-enhanced ionic motion is of great significance, since it will provide clues for the developed perovskite materials with increased stability for device applications. Therefore, the target perovskite for light excitation was changed to $MAPbBr_3$, $MAPb(I_{0.9}Br_{0.1})_3$, and $CsPbI_2Br$ by Zhou *et al* [83]. In $MAPbBr_3$ and $MAPb(I_{0.9}Br_{0.1})_3$ films, plane dendritic structures were still observed under stronger light, indicating halide anions are not the culprits for light-enhanced ion migration. However, with $CsPbI_2Br$ in the same structure, they found that even the light intensities increased to 25 mW cm^{-2}, the perovskite film showed no obvious change and there was no light-induced phase segregation, which is consistent with results by Beal *et al* [48] and implies the suppressed ion migration by Cs substitution. Then, the activation energy for ion migration in $CsPbI_2Br$ was extracted by galvanostatic measurement (figure 6(d)). In comparison with $MAPbI_3$, the barrier for ion migration of Cs-perovskite remains constant (0.45 eV) under growing light intensities, indicating the light-independent ionic transport in all-inorganic perovskite film. This finding strongly implies the key role of the organic cation in the complicated interaction between photo excitation and ion migration since organic cation-based perovskite film demonstrates light-enhanced ion migration. Therefore, Cs substitution is an effective method to suppress the cation migration [84–86].

Kim *et al* found that bromide substitution could strongly weaken the ionic conductivity enhancement in $APbI_3$ ($A = MA^+$, FA^+ or Cs^+) under illumination, however, the variations of A-site cations make a trivial impact on light effects. In PSCs, ion migration is not simply equal to the moving of charged defects. Rather, there is a dynamic interaction between carriers, traps and mobile ions, of which all could be the factor affecting ionic conductivities. For a perovskite film with a larger quantity of vacant defects, the interstitial ions could move and fill them at the initial stage of the ion migration process, during which the 'healing effects' [79] will reduce the number of mobile ions, then lower the ionic conductivities. Additionally, the defect state densities of iodine- and bromide-based perovskite film may exhibit significant variation, on which the ionic conductivities heavily depend. Therefore, we can just spike the conclusion that if the bromide-based perovskite contains a higher amount of vacant defect state densities, more charged ions could compensate them and reduce the ionic conductivities temporarily. Although

Table 1. Summary of the activation energies extracted from the ionic/electronic conductivities under different light intensities for $MAPbI_3$. Reproduced from [69]. CC BY 4.0.

Light intensity (mW cm^{-2})	E_{a1}($T > 250$ k) (meV)	E_{a2}($180 < T < 250$ k) (meV)	E_a(electronic) (meV)
0	Null	134	92
0.05	824	84	84
1	851	63	73
5	334	Null	44
20	144	Null	53

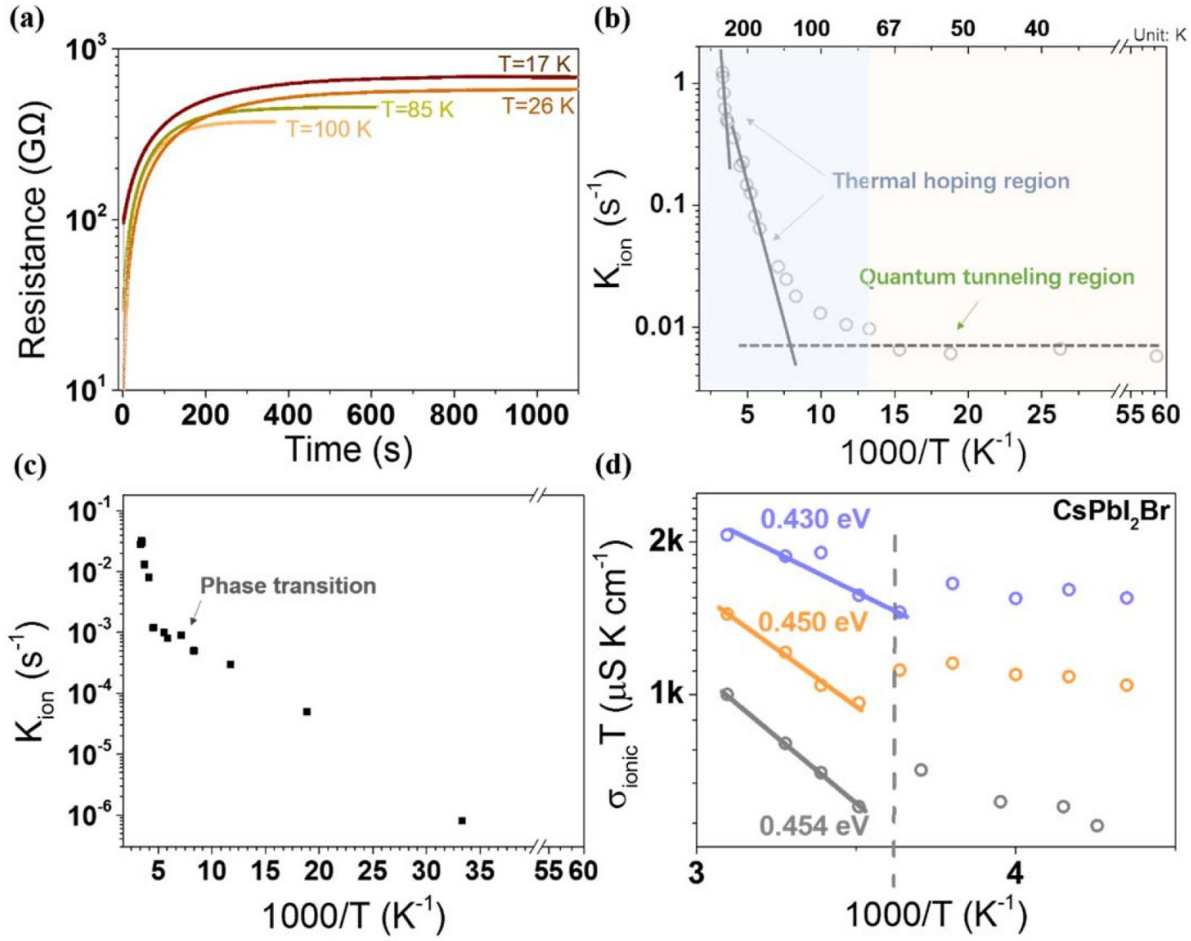

Figure 6. (a) Galvanostatic curves of the ionic conductance at temperatures (17 K–100 K) for the $MAPbI_3$ sample, from which the ionic kinetic constant is derived from exponential fitting for these curves. (b) The ionic kinetic constants vs T for the $MAPbI_3$ perovskite sample. (c) The ionic kinetic constants vs T for $CsPbI_2Br$ perovskite sample. Reprinted with permission from [82]. Copyright 2018 American Chemical Society. (d) Ionic conductivity of $CsPbI_2Br$ films, $\sigma_{ion}T$, as a function of T, under different light intensities (grey: 0.1 mW cm^{-2}; orange: 5 mW cm^{-2}; purple: 25 mW cm^{-2}). Reprinted with permission from [83]. Copyright 2017 American Chemical Society.

ions can heal part of the defects at the early stage of migration, however, prolonged ion migration can cause irreversible changes in perovskite with a large number of defect states near the electrodes, indicated by quenched fluorescence, and eventually cause the solar cells to become unstable.

4.4. Grain boundary and grain size

In solid-state films, ionic motion must be conveyed by the defect states. More defect states means a higher possibility for ion migration. Apart from bulk point defects, GBs could act as pathways for ion migration, due to the high densities of lattice dislocation [87], grain disorientation [88], excess volume [89], impurities segregation [90] and wrong bonds at GBs [91]. Since the state-of-the-art PSCs are fabricated by a low temperate solution process (<150 °C), the target film has a large amount of GBs [92]. Although the defects states located at GBs may not act as deep-level traps, however, they could still boost the hopping-dominated ion migration.

Shao *et al* first discovered a faster ion migration at GBs [93] via comparing the extent of current hysteresis at GBs and in grains of polycrystalline $MAPbI_3$ films (figures 7(a–c)).

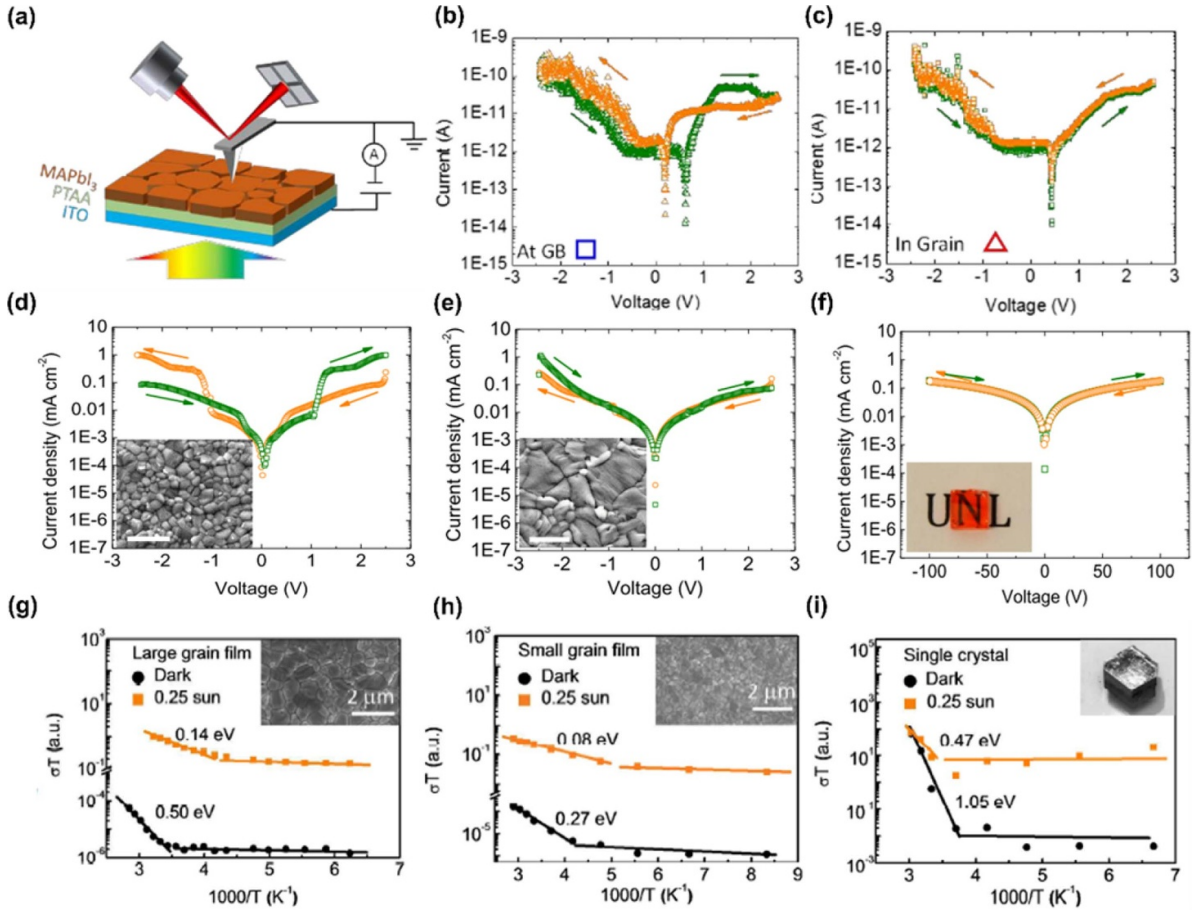

Figure 7. (a) The c-AFM measurement setup to study the ion migration associated local current at GBs and on grains. (b) Local dark current measured at GBs. (c) Local dark current measured in grain. (d)–(f) Grain size-dependent ion migration in perovskite materials measured at macroscopic level. d: small-grain size, e: large-grain size, f: single crystal. The scale bar of SEM image is 2 μm. Reproduced from [93] with permission of The Royal Society of Chemistry. (g)–(i) The temperature-dependent conductivity of a large-grain film (g), a small-grain film (h), and a single crystal (i). The inset pictures of figures 7(g)–(i) are SEM images of tested samples. Reproduced from [80] with permission of The Royal Society of Chemistry.

Then by comparing the extent of hysteresis in perovskite film with different grain sizes, they found that smaller grains could induce more severe *I–V* hysteresis (figures 7(d–f)) and lead to a higher contribution of ionic conductance to the entire conductivities in galvanostatic characterization. Quantitatively, the perovskite film with larger grain size (around 1 μm) exhibited a 0.50 eV (under dark) and 0.14 eV (under light) activation energy for ion migration (figure 7(g)), and in comparison, the value reduced to 0.27 eV and 0.08 eV for perovskite with smaller grains (300 nm) (figure 7(h)), respectively [80]. Sparklingly, the activation energy for ion migration in a single crystal is around 1.10 eV in dark and 0.47 eV under light (figure 7(i)). All the above results reveal that GBs can facilitate the ion migration; therefore, increasing the grain size and passivating defect states at GBs may lead to improved device stability.

4.5. Lattice strain

Due to the formation of GBs and thermal lattice expansion [94, 95] in solid-state crystal, compressive stress and tensile strain are widely distributed in the out-of-plane and in-plane directions of perovskite crystal [96]. Although subsequent thermal annealing can lead to Ostwald ripening [97], which could partly release the strains and reduce GBs densities. However, the residue strains, growing on substrates, can reach 50 MPa [98]. Zhao *et al* qualitatively and quantitatively studied the impact of strain on the stability of $MAPbI_3$ film [99]. First, they curved the film into a convex and a concave shape, to enhance and reduce the lattice strain (figure 8(a)), respectively. After 500 h illumination (50 mW cm^{-2}), a large area of the convex film turned yellow, which is verified to be PbI_2 through XRD measurement (figure 8(b)). In contrast, the concave film was highly stable without any PbI_2 appearance.

The mechanism of strain-accelerated degradation was then discovered to be related to ion migration, given that the perovskite was covered with a thin polystyrene layer to prevent moisture. From the temperature-dependent conductance measurement, the convex, flat and concave $MAPbI_3$ films show gradually enlarged activation energy, which are 0.29 eV, 0.39 eV, 0.53 eV in the dark and 0.046 eV, 0.074 eV, 0.083 eV under 25 mW cm^{-2}, respectively (figures 8(c–f)). Convex

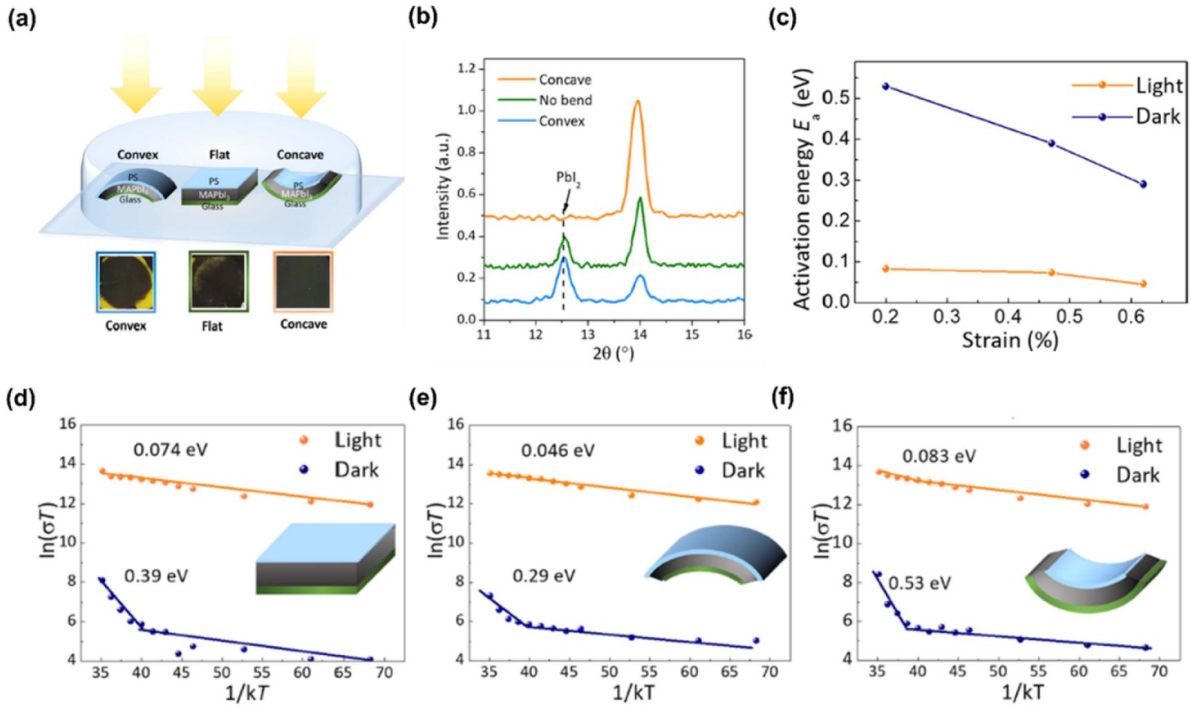

Figure 8. (a) Schematic diagram of the experimental setup of the films with different strains and photographs of the films with different strains after 500 h illumination. (b) Out-of-plane XRD of the three films in (a). (c) Variation of the activation energy of ion migration versus the strain in the $MAPbI_3$ films. (d)–(f) The temperature-dependent conductivity of the convex film (d), the flat film (e), and the concave film (f). Inset: Schematic diagram of the samples. From [99]. Reprinted with permission from AAAS.

film shows the smallest activation energy, which means the most severe ion migration. The results also agree well with the light-enhanced ion migration by showing much smaller activation energy under light compared to darkness. Additionally, Saidaminov *et al* demonstrated that local lattice strain could facilitate the formation of vacancy defects and be detrimental to device stability. Therefore, strain-accelerated ion migration is responsible for the faster degradation in convex film, and sheds light on a path to improve perovskite stability.

It is worth mentioning that Chen *et al* discovered a 1% response of compressive strain in a $MAPbI_3$ single crystal under an electric field of 3.7 V μm^{-1} [100]. Based on the second order relationship between strain response and applied voltage ($S \sim M^2$), the electromechanical response is caused by electrostriction, not the piezoelectric effect, which is a first order coupling. Then, after carefully analyzing several possible mechanisms, like anharmonic displacement of positive/negative ions, Maxwell stress and MA^+ cation ordering, ion/defect migration was considered to be responsible for the electrostrictive response. Finally, they estimated about 0.01%–0.03% compressive strain could be generated in a typical PSC with a built-in field of around 0.3–0.65 V μm^{-1}. Due to the cooling process of $MAPbI_3$ crystal formation, mismatched thermal expansion can lead to residue tensile strain (about 0.47%) in the in-plane direction. Thus, the electrostriction can result in a larger lattice in the in-plane direction, which will then reduce the tensile strain and improve the device stability.

5. Strategy to inhibit ion migration in perovskite film and device

It had been robustly demonstrated that ion migration could raise the defect states in perovskite crystal, cause interfacial band mismatch and lead to HTL degradation. Additionally, anomalous effects, such as *I–V* hysteresis, light-induced phase segregation, and light-induced poling effect, are correlated with ion migration. Therefore, the strategy of inhibiting/suppressing ion migration is very important to improve the stability of the device.

First, based on the solution fabrication process of perovskite film, the formation energy of a defect is relatively low [36–40]. Thus, film contains a large amount of defect states (10^{15} cm^{-3} to 10^{19} cm^{-3}). Due to the defects' hopping-dominated process, defect engineering in the bulk and at the surface is crucial; and recent studies showed that increasing the formation energy of defect states might be an efficient way. Due to the soft tolerant structure of perovskite lattice, many cations and anions could be incorporated into the perovskite crystal. For example, Saliba *et al* first used a triple-cation (MA/FA/Cs) to enhance the device stability [84], followed by incorporating Rb cations in the perovskite film [101]. Additionally, Kim *et al* doped potassium ions to inhibit the ion migration [102]. Because of the tiny radius of K^+, it could just be incorporated into the surface of perovskite grains, mainly lowering the surface defect states. Then, based on the DFT calculation published by Saidaminov *et al*, the substitution of

cations and anions could increase the energetic cost associated with the formation of vacancies and release the lattice strain, thus, inhibiting the ion migration [103]. Recently, Bai *et al* incorporated a tiny amount of ionic liquid ($BMIMBF_4$) and found suppressed ion migration in the target perovskite film [104].

Additionally, blocking the channel for ion migration is another efficient strategy. Post passivation, like PCBM treatment, could reduce the ion diffusion by blocking the GB channels, as well as strengthening the bonding [105]. Similarly, incorporating cations with longer molecular chains to form a 2.5D perovskite structure can also enhance the activation energy for ion migration [106].

In comparison with the high tolerance to defect states of bulk crystal, the interface of PSCs is more sensitive to defect states. Thus, interfacial passivation is also vital to enhance stability. Tan *et al* performed a Cl-passivated TiO_2 fabrication method to obtain a stronger binding at the perovskite/TiO_2 interface and suppress the interfacial recombination with enhanced stability [107]. Similarly, in the solution-processed field-effect transistors (FETs), Wang *et al* demonstrates the decrease in ion migration by modifying the Au/perovskite interface [108].

6. Summary and outlook

Generally, the operational stability of typical PSCs cannot currently meet the commercial standards. Solving the instability problem is the first step towards commercialization of PSCs. As concluded in the previous sections, ion migration could generate defects states in perovskite bulk crystal, induce interfacial band doping and destroy the organic HTL, which intrinsically influence the stability of the solar cell device. Due to the photoactive, organic–cationic, solution-processed and polycrystalline nature of perovskite materials, light illumination/organic cations/GBs/tensile strain have been found to affect ion migration to some degree, and further affect the stability of PSCs. Accordingly, various strategies could be developed to suppress ion migration toward highly stable PSCs. For the perovskite layer, one can lower defect state densities, enlarge grain size, increase cesium content; and for carrier transport materials, an ion-blocking layer may be beneficial.

To thoroughly understand the ion migration in PSCs, many open questions still need to be addressed, such as: (1) How should the migration of cations and anions be characterized at the atomic and molecular scale independently? The state-of-art characterization cannot distinguish such migrated species microscopically. (2) What is the mechanism behind light-enhanced ion migration phenomena? Light is essential to photovoltaic devices, and it is urgent to understand the photon–phonon interaction. (3) How can the ion migration be suppressed without sacrificing the efficiency of PSCs? After uncovering the deep mechanism for ion migration, ion migration is believed to be effectively regulated in perovskite film, based on different requirements.

From the perspective of developing the photovoltaic industry, in our view, one direction is to develop inorganic PSCs, in which ion migration has been demonstrated to be light-independent. However, the performance of inorganic PSCs is far behind those with organic species, like MA^+ and FA^+. Poor carrier lifetime and low phase stability of inorganic perovskite film are the origin, which can be modified by component regulation and interface passivation. Another option is to develop silicon/perovskite heterojunction tandem solar cells with an optimum bandgap of 1.75 eV for the perovskite part. Tandem cells could improve the device efficiency to around 30%. However, the present key point is to improve the open-circuit voltage of wide-bandgap PSCs, of which the current–voltage loss is beyond 0.6 V, far behind the Shockley–Queisser limit. If stable tandem silicon/PSCs could be achieved with a V_{oc} of 1.3 V and a J_{sc} of 18 mA cm^{-2}, PSCs could win a seat on the board of the photovoltaic industry in the future.

Acknowledgments

This work is supported by National Key Research and Development Program of China (Grant No. 2019YFA0707003), the National Natural Science Foundation of China (Grant Nos. NSFC 91733301, 51872007) and Beijing Municipal Natural Science Foundation (Grant No. 7202094).

Conflict of interest

The authors declare no competing interests.

ORCID iDs

Zhiqian Yang https://orcid.org/0000-0002-3132-1777
Qing Zhao https://orcid.org/0000-0003-3374-6901

References

[1] Green M A, Ho-Baillie A and Snaith H J 2014 The emergence of perovskite solar cells *Nat. Photonics* **8** 506–14
[2] Stranks S D, Eperon G E, Grancini G, Menelaou C, Alcocer M J P, Leijtens T, Herz L M, Petrozza A and Snaith H J 2013 Electron-hole diffusion lengths exceeding 1 micrometer in an organometal trihalide perovskite absorber *Science* **342** 341–4
[3] Dong Q, Fang Y, Shao Y, Mulligan P, Qiu J, Cao L and Huang J 2015 Electron-hole diffusion lengths > 175 μm in solution-grown $CH_3NH_3PbI_3$ single crystals *Science* **347** 967–70
[4] McGehee M D 2014 Continuing to Soar *Nat. Mater.* **13** 845–6
[5] Zhao D *et al* 2017 Low-bandgap mixed tin–lead iodide perovskite absorbers with long carrier Lifetimes for all-perovskite tandem solar cells *Nat. Energy* **2** 17018
[6] Shi D *et al* 2015 Low trap-state density and long carrier diffusion in organolead trihalide perovskite single crystals *Science* **347** 519–22
[7] National Renewable Energy Laboratory, Golden, CA 2020 Best research-cell efficiency chart (United States)

[8] Burschka J, Pellet N, Moon S-J, Humphry-Baker R, Gao P, Nazeeruddin M K and Grätzel M 2013 Sequential deposition as a route to high-performance perovskite-sensitized solar cells *Nature* **499** 316–9

[9] Liu D and Kelly T L 2014 Perovskite solar cells with a planar heterojunction structure prepared using room-temperature solution processing techniques *Nat. Photonics* **8** 133–8

[10] Yang M *et al* 2017 Perovskite ink with wide processing window for scalable high-efficiency solar cells *Nat. Energy* **2** 17038

[11] Kieslich G, Sun S and Cheetham A K 2015 An extended tolerance factor approach for organic–inorganic perovskites *Chem. Sci.* **6** 3430–3

[12] Stoumpos C C, Malliakas C D and Kanatzidis M G 2013 Semiconducting tin and lead iodide perovskites with organic cations: phase transitions, high mobilities, and near-infrared photoluminescent properties *Inorg. Chem.* **52** 9019–38

[13] Noh J H, Im S H, Heo J H, Mandal T N and Seok S I 2013 Chemical management for colorful, efficient, and stable inorganic–organic hybrid nanostructured solar cells *Nano Lett.* **13** 1764–9

[14] Eperon G E, Stranks S D, Menelaou C, Johnston M B, Herz L M and Snaith H J 2014 Formamidinium lead trihalide: a broadly tunable perovskite for efficient planar heterojunction solar cells *Energy Environ. Sci.* **7** 982–8

[15] Pellet N, Gao P, Gregori G, Yang T-Y, Nazeeruddin M K, Maier J and Grätzel M 2014 Mixed-organic-cation perovskite photovoltaics for enhanced solar-light harvesting *Angew. Chem. Int. Ed.* **53** 3151–7

[16] Filip M R, Eperon G E, Snaith H J and Giustino F 2014 Steric engineering of metal-halide perovskites with tunable optical band gaps *Nat.Commun.* **5** 5757

[17] Sahli F *et al* 2018 Fully textured monolithic perovskite/silicon tandem solar cells with 25.2% power conversion efficiency *Nat. Mater.* **17** 820–6

[18] Deng Y, Van Brackle C H, Dai X, Zhao J, Chen B and Huang J 2019 Tailoring solvent coordination for high-speed, room-temperature blading of perovskite photovoltaic films *Sci. Adv.* **5** eaax7537

[19] Boyd C C, Cheacharoen R, Leijtens T and McGehee M D 2018 Understanding degradation mechanisms and improving stability of perovskite photovoltaics *Chem. Rev.* **119** 3418–51

[20] Leijtens T, Eperon G E, Noel N K, Habisreutinger S N, Petrozza A and Snaith H J 2015 Stability of metal halide perovskite solar cells *Adv. Energy Mater.* **5** 1500963

[21] Zhao Y, Wei J, Li H, Yan Y, Zhou W, Yu D and Zhao Q 2016 A polymer scaffold for self-healing perovskite solar cells *Nat.Commun.* **7** 10228

[22] Yang J, Siempelkamp B D, Liu D and Kelly T L 2015 Investigation of $CH_3NH_3PbI_3$ degradation rates and mechanisms in controlled humidity environments using *in situ* techniques *ACS Nano* **9** 1955–63

[23] Aristidou N, Eames C, Sanchez-Molina I, Bu X, Kosco J, Islam M S and Haque S A 2017 Fast oxygen diffusion and iodide defects mediate oxygen-induced degradation of perovskite solar cells *Nat.Commun.* **8** 15218

[24] Divitini G, Cacovich S, Matteocci F, Cinà L, Di Carlo A and Ducati C 2016 *In situ* observation of heat-induced degradation of perovskite solar cells *Nat. Energy* **1** 15012

[25] Leijtens T, Eperon G E, Pathak S, Abate A, Lee M M and Snaith H J 2013 Overcoming ultraviolet light instability of sensitized TiO_2 with meso-superstructured organometal tri-halide perovskite solar cells *Nat.Commun.* **4** 2885

[26] Walsh A 2015 Principles of chemical bonding and band gap engineering in hybrid organic–inorganic halide perovskites *J. Phys. Chem.* C **119** 5755–60

[27] Xiao Z, Yuan Y, Shao Y, Wang Q, Dong Q, Bi C, Sharma P, Gruverman A and Huang J 2015 Giant switchable photovoltaic effect in organometal trihalide perovskite devices *Nat. Mater.* **14** 193–8

[28] Juarez-Perez E J, Sanchez R S, Badia L, Garcia-Belmonte G, Kang Y S, Mora-Sero I and Bisquert J 2014 Photoinduced giant dielectric constant in lead halide perovskite solar cells *J. Phys. Chem. Lett.* **5** 2390–4

[29] Hoke E T, Slotcavage D J, Dohner E R, Bowring A R, Karunadasa H I and McGehee M D 2015 Reversible photo-induced trap formation in mixed-halide hybrid perovskites for photovoltaics *Chem. Sci.* **6** 613–7

[30] Deng Y, Xiao Z and Huang J 2015 Light-induced self-poling effect on organometal trihalide perovskite solar cells for increased device efficiency and stability *Adv. Energy Mater.* **5** 1500721

[31] Snaith H J, Abate A, Ball J M, Eperon G E, Leijtens T, Noel N K, Stranks S D, Wang J T-W, Wojciechowski K and Zhang W 2007 Anomalous hysteresis in perovskite solar cells *J. Phys. Chem. Lett.* **5** 1511–5

[32] Mizusaki J, Arai K and Fueki K 1983 Ionic conduction of the perovskite-type halides *Solid State Ion* **11** 203–11

[33] Yang T-Y, Gregori G, Pellet N, Grätzel M and Maier J 2015 The significance of ion conduction in a hybrid organic–inorganic Lead-Iodide-based perovskite photosensitizer *Angew. Chem. Int. Ed.* **54** 7905–10

[34] Tress W, Marinova N, Moehl T, Zakeeruddin S M, Nazeeruddin M K and Grätzel M 2015 Understanding the rate-dependent J–V hysteresis, slow time component, and aging in $CH_3NH_3PbI_3$ perovskite solar cells: the role of a compensated electric field *Energy Environ. Sci.* **8** 995–1004

[35] Li C-S, Cheng T-C, Shen S-W, Wu Y-T, Cheng J-R, Ni I C, Chen M-H and Wu C-I 2019 Influence of work function of carrier Transport Mater. With Perovskite on Switchable Photovoltaic Phenomena *J. Phys. Chem.* C **123** 28668–76

[36] Yan Y and Wei S-H 2008 Doping asymmetry in wide-bandgap semiconductors: origins and solutions *Phys. Status Solidi* B **245** 641–52

[37] Wei S-H 2004 Overcoming the doping bottleneck in semiconductors *Comput. Mater. Sci.* **30** 337–48

[38] Yin W-J, Shi T and Yan Y 2014 Unusual defect physics in $CH_3NH_3PbI_3$ perovskite solar cell absorber *Appl. Phys. Lett.* **104** 063903

[39] Wang Q, Shao Y, Xie H, Lyu L, Liu X, Gao Y and Huang J 2014 Qualifying composition dependent P and N self-doping in $CH_3NH_3PbI_3$ *Appl. Phys. Lett.* **105** 163508

[40] Shi T, Yin W-J, Hong F, Zhu K and Yan Y 2015 Unipolar self-doping behavior in perovskite $CH_3NH_3PbBr_3$ *Appl. Phys. Lett.* **106** 103902

[41] Eames C, Frost J M, Barnes P R F, O'Regan B C, Walsh A and Islam M S 2015 Ionic transport in hybrid lead iodide perovskite solar cells *Nat.Commun.* **6** 7497

[42] Chen B, Yang M, Priya S and Zhu K 2016 Origin of J–V hysteresis in perovskite solar cells *J. Phys. Chem. Lett.* **7** 905–17

[43] Haruyama J, Sodeyama K, Han L and Tateyama Y 2015 First-principles study of ion diffusion in perovskite solar cell sensitizers *J. Am. Chem. Soc.* **137** 10048–51

[44] Yuan Y, Chae J, Shao Y, Wang Q, Xiao Z, Centrone A and Huang J 2015 Photovoltaic switching mechanism in lateral structure hybrid perovskite solar cells *Adv. Energy Mater.* **5** 1500615

[45] Yuan Y, Wang Q, Shao Y, Lu H, Li T, Gruverman A and Huang J 2016 Electric-field-driven reversible conversion between methylammonium lead triiodide perovskites and lead iodide at elevated temperatures *Adv. Energy Mater.* **6** 1501803

[46] Egger D A, Kronik L and Rappe A M 2015 Theory of hydrogen migration in organic–inorganic halide perovskites *Angew. Chem. Int. Ed.* **54** 12437–41

[47] Li C, Tscheuschner S, Paulus F, Hopkinson P E, Kießling J, Köhler A, Vaynzof Y and Huettner S 2016 Iodine migration and its effect on hysteresis in perovskite solar cells *Adv. Mater.* **28** 2446–54

[48] Beal R E, Slotcavage D J, Leijtens T, Bowring A R, Belisle R A, Nguyen W H, Burkhard G F, Hoke E T and McGehee M D 2016 Cesium lead halide Perovskites with improved stability for tandem solar cells *J. Phys. Chem. Lett.* **7** 746–51

[49] Zhao Y, Zhou W, Ma W, Meng S, Li H, Wei J, Fu R, Liu K, Yu D and Zhao Q 2016 Correlations between immobilizing ions and suppressing hysteresis in perovskite solar cells *ACS Energy Lett.* **1** 266–72

[50] Kuokstis E, Yang J W, Simin G, Khan M A, Gaska R and Shur M S 2002 Two mechanisms of blueshift of edge emission in InGaN-based epilayers and multiple quantum wells *Appl. Phys. Lett.* **80** 977–9

[51] Eliseev P G, Perlin P, Lee J and Osiński M 1997 'Blue' temperature-induced shift and band-tail emission in InGaN-based light sources *Appl. Phys. Lett.* **71** 569–71

[52] Zhou W, Chen S, Zhao Y, Li Q, Zhao Y, Fu R, Yu D, Gao P and Zhao Q 2019 Constructing $CsPbBr_3$ cluster passivated-triple cation perovskite for highly efficient and operationally stable solar cells *Adv. Funct. Mater.* **29** 1809180

[53] Mönch W 2001 *Semiconductor Surfaces and Interfaces* (Berlin: Springer)

[54] Marin-Beloqui J M, Lanzetta L and Palomares E 2016 Decreasing charge losses in perovskite solar cells through mp-TiO_2/MAPI interface engineering *Chem. Mater.* **28** 207–13

[55] Guerrero A, Marchesi L F, Boix P P, Ruiz-Raga S, Ripolles-Sanchis T, Garcia-Belmonte G and Bisquert J 2012 How the charge-neutrality level of interface states controls energy level alignment in cathode contacts of organic bulk-heterojunction solar cells *ACS Nano* **6** 3453–60

[56] Seol D-J, Lee J-W and Park N-G 2015 On the role of interfaces in planar-structured $HC(NH_2)_2PbI_3$ perovskite solar cells *Chem. Sus. Chem.* **8** 2414–9

[57] Zhou H, Chen Q, Li G, Luo S, Song T-B, Duan H-S, Hong Z, You J, Liu Y and Yang Y 2014 Interface engineering of highly efficient perovskite solar cells *Science* **345** 542–6

[58] Zhang H, Liang C, Zhao Y, Sun M, Liu H, Liang J, Li D, Zhang F and He Z 2015 Dynamic interface charge governing the current–voltage hysteresis in perovskite solar cells *Phys. Chem. Chem. Phys.* **17** 9613–8

[59] Zhao Y *et al* 2015 Anomalously large interface charge in polarity-switchable photovoltaic devices: an indication of mobile ions in organic–inorganic halide perovskites *Energy Environ. Sci.* **8** 1256–60

[60] Kim J, Lee S-H, Lee J H and Hong K-H 2014 The role of intrinsic defects in methylammonium lead iodide perovskite *J. Phys. Chem. Lett.* **5** 1312–7

[61] Zhao Y, Zhou W, Tan H, Fu R, Li Q, Lin F, Yu D, Walters G, Sargent E H and Zhao Q 2017 Mobile-ion-induced degradation of organic hole-selective layers in perovskite solar cells *J. Phys. Chem.* C **121** 14517–23

[62] Correa-Baena J-P *et al* 2017 Identifying and suppressing interfacial recombination to achieve high open-circuit voltage in perovskite solar cells *Energy Environ. Sci.* **10** 1207–12

[63] Tavakoli M M, Tress W, Milić J V, Kubicki D, Emsley L and Grätzel M 2018 Addition of adamantylammonium iodide to hole transport layers enables highly efficient and electroluminescent perovskite solar cells *Energy Environ. Sci.* **11** 3310–20

[64] Liu Z *et al* 2018 Open-circuit voltages exceeding 1.26 V in planar methylammonium lead iodide perovskite solar cells *ACS Energy Lett.* **4** 110–7

[65] Luo D *et al* 2018 Enhanced photovoltage for inverted planar heterojunction perovskite solar cells *Science* **360** 1442–6

[66] Nie W *et al* 2016 Light-activated photocurrent degradation and self-healing in perovskite solar cells *Nat. Commun.* **7** 11574

[67] Pockett A, Eperon G E, Sakai N, Snaith H J, Peter L M and Cameron P J 2017 Microseconds, milliseconds and seconds: deconvoluting the dynamic behaviour of planar perovskite solar cells *Phys. Chem. Chem. Phys.* **19** 5959–70

[68] Leijtens T *et al* 2015 Mapping electric field-induced switchable poling and structural degradation in hybrid lead halide perovskite thin films *Adv. Energy Mater.* **5** 1500962

[69] Zhao Y-C, Zhou W-K, Zhou X, Liu K-H, Yu D-P and Zhao Q 2017 Quantification of light-enhanced ionic transport in lead iodide perovskite thin films and its solar cell applications *Light Sci. Appl.* **6** e16243

[70] Domanski K, Alharbi E A, Hagfeldt A, Grätzel M and Tress W 2018 Systematic investigation of the impact of operation conditions on the degradation behaviour of perovskite solar cells *Nat. Energy* **3** 61–67

[71] Bryant D, Aristidou N, Pont S, Sanchez-Molina I, Chotchunangatchaval T, Wheeler S, Durrant J R and Haque S A 2016 Light and oxygen induced degradation limits the operational stability of methylammonium lead triiodide perovskite solar cells *Energy Environ. Sci.* **9** 1655–60

[72] Morimoto T, Nagai M, Minowa Y, Ashida M, Yokotani Y, Okuyama Y and Kani Y 2019 Microscopic ion migration in solid electrolytes revealed by terahertz time-domain spectroscopy *Nat. Commun.* **10** 2662

[73] León C, Rivera A, Várez A, Sanz J, Santamaria J and Ngai K L 2001 Origin of constant loss in ionic conductors *Phys. Rev. Lett.* **86** 1279–82

[74] Koettgen J, Zacherle T, Grieshammer S and Martin M 2017 *Ab initio* calculation of the attempt frequency of oxygen diffusion in pure and samarium doped ceria *Phys. Chem. Chem. Phys.* **19** 9957–73

[75] Jones A, Slater P R and Islam M S 2008 Local defect structures and ion transport mechanisms in the oxygen-excess apatite $La_{9.67}(SiO_4)_6O_{2.5}$ *Chem. Mater.* **20** 5055–60

[76] Islam M S, Driscoll D J, Fisher C A J and Slater P R 2005 Atomic-scale investigation of defects, dopants, and lithium transport in the $LiFePO_4$ olivine-type battery material *Chem. Mater.* **17** 5085–92

[77] Yokota I 1961 On the theory of mixed conduction with special reference to conduction in silver sulfide group semiconductors *J. Phys. Soc. Japan* **16** 2213–23

[78] Yokota I 1953 On the electrical conductivity of cuprous sulfide: a diffusion theory *J. Phys. Soc. Japan* **8** 595–602

[79] deQuilettes D W, Zhang W, Burlakov V M, Graham D J, Leijtens T, Osherov A, Bulović V, Snaith H J, Ginger D S and Stranks S D 2016 Photo-induced halide redistribution in organic–inorganic perovskite films *Nat. Commun.* **7** 11683

[80] Xing J, Wang Q, Dong Q, Yuan Y, Fang Y and Huang J 2016 Ultrafast ion migration in hybrid perovskite polycrystalline thin films under light and suppression in single crystals *Phys. Chem. Chem. Phys.* **18** 30484–90

[81] Kim G Y, Senocrate A, Yang T-Y, Gregori G, Grätzel M and Maier J 2018 Large tunable photoeffect on ion conduction in halide perovskites and implications for photodecomposition *Nat. Mater.* **17** 445–9

[82] Feng Y, Zhao Y, Zhou W-K, Li Q, Saidi W A, Zhao Q and Li X-Z 2018 Proton migration in hybrid lead iodide perovskites: from classical hopping to deep quantum tunneling *J. Phys. Chem. Lett.* **9** 6536–43
[83] Zhou W, Zhao Y, Zhou X, Fu R, Li Q, Zhao Y, Liu K, Yu D and Zhao Q 2017 Light-independent ionic transport in inorganic perovskite and ultrastable Cs-based perovskite solar cells *J. Phys. Chem. Lett.* **8** 4122–8
[84] Saliba M *et al* 2016 Cesium-containing triple cation perovskite solar cells: improved stability, reproducibility and high efficiency *Energy Environ. Sci.* **9** 1989–97
[85] Zhao Y *et al* 2018 Perovskite seeding growth of formamidinium-lead-iodide-based perovskites for efficient and stable solar cells *Nat. Commun.* **9** 1607
[86] Li Q, Zhao Y, Fu R, Zhou W, Zhao Y, Liu X, Yu D and Zhao Q 2018 Efficient perovskite solar cells fabricated through CsCl-enhanced PbI_2 precursor via sequential deposition *Adv. Mater.* **30** 1803095
[87] Read W T and Shockley W 1950 Dislocation models of crystal grain boundaries *Phys. Rev.* **78** 275–89
[88] Brandon D G 1966 The structure of high-angle grain boundaries *Acta Metall.* **14** 1479–84
[89] Pond R C 1979 The measurement of excess volume at grain boundaries using transmission electron microscopy *J. Microsc.* **116** 105–14
[90] Yamaguchi M, Shiga M and Kaburaki H 2005 Grain boundary decohesion by impurity segregation in a nickel-sulfur system *Science* **307** 393–7
[91] Lambrecht W R L, Lee C H, Methfessel M, Van Schilfgaarde M, Amador C and Segall B 1990 Wrong bonds at compound semiconductor grain boundaries *MRS Proc.* **209** 667
[92] Long R, Liu J and Prezhdo O V 2016 Unravelling the effects of grain boundary and chemical doping on electron–hole recombination in $CH_3NH_3PbI_3$ perovskite by time-domain atomistic simulation *J. Am. Chem. Soc.* **138** 3884–90
[93] Shao Y *et al* 2016 Grain boundary dominated ion migration in polycrystalline organic–inorganic halide perovskite films *Energy Environ. Sci.* **9** 1752–9
[94] Schueller E C, Laurita G, Fabini D H, Stoumpos C C, Kanatzidis M G and Seshadri R 2018 Crystal structure evolution and notable thermal expansion in hybrid perovskites formamidinium tin Iodide and formamidinium lead bromide *Inorg. Chem.* **57** 695–701
[95] Jacobsson T J, Schwan L J, Ottosson M, Hagfeldt A and Edvinsson T 2015 Determination of thermal expansion coefficients and locating the temperature-induced phase transition in methylammonium lead perovskites using x-ray diffraction *Inorg. Chem.* **54** 10678–85
[96] Steele J A *et al* 2019 Thermal unequilibrium of strained black $CsPbI_3$ thin films *Science* **365** 679–84
[97] Yang Y *et al* 2020 Suppressing vacancy defects and grain boundaries via ostwald ripening for high-performance and stable perovskite solar cells *Adv. Mater.* **32** 1904347
[98] Rolston N, Bush K A, Printz A D, Gold-Parker A, Ding Y, Toney M F, McGehee M D and Dauskardt R H 2018 Engineering stress in perovskite solar cells to improve stability *Adv. Energy Mater.* **8** 1802139
[99] Zhao J, Deng Y, Wei H, Zheng X, Yu Z, Shao Y, Shield J E and Huang J 2017 Strained hybrid perovskite thin films and their impact on the intrinsic stability of perovskite solar cells *Sci. Adv.* **3** eaao5616
[100] Chen B *et al* 2018 Large electrostrictive response in lead halide perovskites *Nat. Mater.* **17** 1020–6
[101] Saliba M *et al* 2016 Incorporation of rubidium cations into perovskite solar cells improves photovoltaic performance *Science* **354** 206–9
[102] Kim S-G, Li C, Guerrero A, Yang J, Zhong Y, Bisquert J, Huettner S and Park N-G 2019 Potassium ions as a kinetic controller in ionic double layers for hysteresis-free perovskite solar cells *J. Mater. Chem.* A **7** 18807–15
[103] Saidaminov M I *et al* 2018 Suppression of atomic vacancies via incorporation of isovalent small ions to increase the stability of halide perovskite solar cells in ambient air *Nat. Energy* **3** 648–54
[104] Bai S *et al* 2019 Planar perovskite solar cells with long-term stability using ionic liquid additives *Nature* **571** 245–50
[105] Zhong Y, Hufnagel M, Thelakkat M, Li C and Huettner S 2020 Role of PCBM in the suppression of hysteresis in perovskite solar cells *Adv. Funct. Mater.* **30** 1908920
[106] Li C, Wang N, Guerrero A, Zhong Y, Long H, Miao Y, Bisquert J, Wang J and Huettner S 2019 Understanding the improvement in the stability of a self-assembled multiple-quantum well perovskite light-emitting diode *J. Phys. Chem. Lett.* **10** 6857–64
[107] Tan H *et al* 2017 Efficient and stable solution-processed planar perovskite solar cells via contact passivation *Science* **355** 722–6
[108] Wang J *et al* 2019 Investigation of electrode electrochemical reactions in $CH_3NH_3PbBr_3$ perovskite single-crystal field-effect transistors *Adv. Mater.* **31** 1902618